Proceedings of ERAD 2006

Assessment of polarimetric rain rate algorithms at C-band frequencies

Miguel Angel Rico-Ramirez and Ian David Cluckie

Dept. of Civil Engineering, University of Bristol, Bristol, BS8 1UP, UK.

Abstract. The purpose of this paper is to evaluate the performance of different polarimetric rainfall estimation algorithms at C-band frequencies. The polarimetric rainfall algorithms are obtained using a wide range of measured drop size distributions with an optical disdrometer in the UK. A dense network of raingauges was used to validate the polarimetric rainfall estimates and the overall results were compared with the conventional Marshall and Palmer relationship. The uncertainty in the rainfall estimation due to noise in the polarimetric radar measurements is also addressed in this paper.

1 Introduction

Physically-based rain estimator algorithms rely on scattering simulations of raindrops without any feedback from rain gauge measurements (Bringi and Chandrasekar, 2001). The scattering simulations of a single oblate raindrop can be computed using the T-matrix approach (See e.g. Mishchenko, 2000), assuming a wide range of Drop Size Distributions (DSD) and a given drop deformation formula (axial ratio versus diameter). Then, the horizontal reflectivity (Z_h), the differential reflectivity (Z_{dr}), the specific differential phase (K_{dp}) and the rainfall rate (R) can be calculated. The polarimetric rainfall estimator algorithms are obtained by performing a non-linear regression between the known rainfall rate and any combination of the simulated radar measurements Z_h, Z_{dr} and K_{dp}. Some of the early work was carried out by Sachidananda and Zrnic (1987) and they proposed the algorithm $R = aK_{dp}^{b}$ to estimate the rain rate from differential phase measurements. Chandrasekar and Bringi (1988) proposed an algorithm of the form $R = aZ_h^b Z_{dr}^c$ to estimate the rain rate from reflectivity and differential reflectivity measurements and Illingworth and Blackman, (2002) proposed an alternative algorithm of the form $Z / R = a_0 + a_1 Z_{dr} + a_2 Z_{dr}^{\ 2} + a_3 Z_{dr}^{\ 3}$. Bringi and Chandrasekar, (2001) summarised several of these relationships using a particular drop deformation formula. Lee, (2003) pointed out that the random error due to the variation of the drop size distribution can be, in principle, be reduced by using the polarimetric radar observables to estimate the rain rate, but without knowing the precise knowledge on the drop deformation, this advantage is minimized. In this paper, the radar measurements Z_h, Z_{dr} and K_{dp} were simulated using measured DSD. Then, several rain estimator algorithms were proposed using a combination of several widely accepted drop deformation formulae. The expected theoretical errors in the rain estimation were calculated and the results presented in Sections 3-5.

Correspondence to: Miguel Angel Rico-Ramirez.

M.A.Rico-Ramirez@bristol.ac.uk

2 Data

An optical disdrometer (Illingworth and Stevens, 1987) was deployed by the Institute of Hydrology (now CEH Wallingford) during intense observing periods in the Brue catchment in the UK during the Hydrological Radar Experiment (HYREX). The disdrometer measured drop sizes between 0.72 mm and 3.62 mm in 0.21 mm steps, although drop sizes less than 0.72 mm and bigger than 3.62 mm were also detected. The disdrometer sampling time was 10 s and 60 s and the data set covered approximately 15000 samples during 1995. The disdrometer data were used to calculate the DSD in order to simulate Z_h, Z_{dr} and K_{dp}.

The radar data (19-27 May 2006) were obtained from the Thurnham radar located in the South East of England. This new radar system is a multi-parameter C-band radar (λ=5.5 cm) with simultaneous transmission and reception of Horizontal (H) and Vertical (V) polarised waves. This is one of the first operational C-band systems with the power divider and receiver in the pedestal to maximize data quality by minimising sources of systematic error from rotating joints. The radar beam width was 0.95°, with typical gate resolutions of 125 m, 250 m and 500 m and the peak power was 250 kW. The tipping bucket rain gauge data were collected over the Medway catchment, with 73 gauges in total, being located within 50 km radius of the radar site.

3 Radar scattering simulations

Dual-polarisation weather radars transmit H and V polarized electromagnetic waves and receive polarized backscattered signals. The backscattering characteristics of a single precipitation particle are described in terms of the backscattering matrix **S** (Bringi and Chandrasekar, 2001). The polarimetric radar observables are related to the scattering elements of the backscattering matrix and they are defined as follows (See also Aydin, 2000). The reflectivity factors at H and V polarizations are calculated by:

$$Z_{hh,vv} = \frac{\lambda^4}{\pi^5 |K|^2} \int \sigma_{hh,vv}(D) N(D)\, \mathrm{d}D \quad (\mathrm{mm}^6\ \mathrm{m}^{-3}) \qquad (1)$$

where D is the drop diameter, λ is the radar wavelength, $|K|^2$ is the refractive index of the hydrometeors (0.93 for water, Battan, 1973), $\sigma_{hh,vv}(D)$ are the backscattering cross sections at H and V polarizations respectively and $N(D)$ is the DSD. The backscattering cross sections can be expressed in terms of the amplitude matrix elements by:

$$\sigma_{hh,vv} = 4\pi |S_{hh,vv}|^2 \quad (\mathrm{mm}^2) \qquad (2)$$

The differential reflectivity is calculated by:

$$Z_{dr} = 10 \log\left(\frac{Z_{hh}}{Z_{vv}}\right) \quad (\mathrm{dB}) \qquad (3)$$

The specific differential phase is calculated by:

$$K_{dp} = 10^3 \frac{180\lambda}{\pi} \int \mathrm{Re}(f_h - f_v) N(D)\, \mathrm{d}D \quad (\mathrm{deg\ km}^{-1}) \qquad (4)$$

where f_h and f_v are the forward scattering amplitudes for H and V polarised waves. The rain rate is then calculated by:

$$R = \frac{\pi}{6} \int D^3 v(D) N(D)\, \mathrm{d}D \quad (\mathrm{mm\ hr}^{-1}) \qquad (5)$$

where $v(D)$ is the terminal velocity of the raindrops. Atlas and Ulbrich (1977) expressed the terminal velocity as a function of the particle diameter, given by $v(D) = 3.78 D^{0.67}$ m s^{-1}, assuming the absence of vertical air motions. The measured DSD with the optical disdrometer was calculated as (Illingworth and Stevens, 1987):

$$N(D_i) = \frac{t_i}{T V_e \Delta D} \quad (\mathrm{m}^{-3}\ \mathrm{mm}^{-1}) \qquad (6)$$

where D_i is the average size diameter of the drops in class i, t_i is the drop time of flight measured in drop size class i, T is the sampling period, V_e is the effective sampling volume and ΔD is the diameter interval. Eq. 6 has the advantage of being independent of drop fall velocities. The maximal instantaneous rainfall in this data set was 51.25 mm hr^{-1}.

In this paper, the drop deformation formulas proposed by Pruppacher and Beard, (1970), Beard and Chuang, (1987) and Andsager et al., (1999) are used for the scattering simulations. These drop deformation formulas are widely accepted in the literature and they were obtained from laboratory experiments. The scattering simulations are performed assuming a temperature of 10°C, although there are not significant differences in the range 0-25°C (See Holt, 1984). Fig. 1 shows the scattering simulations for oblate raindrops using measured DSDs and different drop deformation formulae. This figure shows that the drop deformation has a large effect on the scattering simulations (See also Lee, 2003) and therefore it is important to develop polarimetric rain rate algorithms that are relatively immune to the precise form of the drop shapes. In this paper, it is proposed to combine the scattering simulations from the three drop deformation models in order to obtain a robust polarimetric algorithm for rainfall estimation.

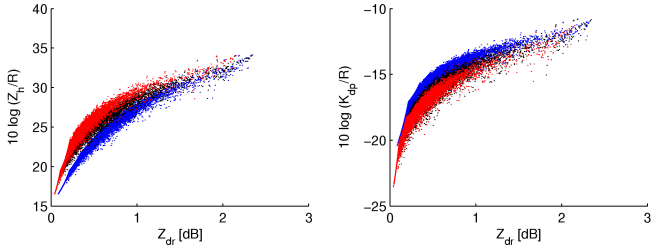

Fig. 1. Radar scattering simulations at C-band frequencies using measured DSDs and assuming the drop shape models of Pruppacher and Beard, (1970), Beard and Chuang, (1987) and Andsager et al., (1999), (blue, black and red dots respectively).

4 Polarimetric algorithms for rainfall estimation

The proposed polarimetric rain rate algorithms obtained by performing a non-linear regression between the known rainfall rate and any combination of the simulated radar measurements are shown in Table 1. The theoretical error between the rainfall and the estimated rainfall with any of these algorithms can be calculated by:

$$e_i = \sqrt{\frac{1}{n}\Sigma\left(R_i - \hat{R}_i\right)^2} \Big/ \frac{1}{n}\Sigma R_i \qquad (7)$$

where R is the computed rainfall rate from the DSD, $\hat{R}$ is the estimated rainfall using any polarimetric algorithm and n is the number of data points having approximately the same rainfall R, but obtained from different DSDs. The estimated rainfall using the conventional Marshall and Palmer (MP) relationship, $Z = 200 R_0^{1.6}$ (Marshall et. al 1955), is also included in the comparisons. Fig 2a shows the expected theoretical errors when using any algorithm shown in Table 1. The MP equation produces the largest errors and the algorithm R_4 the smallest. As shown, all the errors produced by the polarimetric algorithms tend to decrease when increasing the rain rate. However, these errors are obtained in the absence of noise, but in reality this is not the case and the radar measurements are severely affected by noise. Fig 2b shows the errors assuming theoretical levels of white Gaussian noise in the polarimetric radar measurements, that is, $\sigma(Z_h) = 1.0$ dBZ, $\sigma(Z_{dr}) = 0.1$ dB and $\sigma(K_{dp}) = 0.35$ deg km^{-1}. Fig. 2b shows that the noise effects in the radar measurements can heavily influence the rainfall estimation process.

Table 1. Polarimetric rainfall estimator algorithms obtained by combining different drop shape models using measured DSD and valid at C-band frequencies (R<51 mm hr^{-1}). R in mm hr^{-1}, Z_h in mm^6 m^{-3}, Z_{dr} in dB and K_{dp} in deg km^{-1}.

$R_1 = 0.01583 Z_h^{0.8349} 10^{-0.3732 Z_{dr}}$
$R_2 = 0.00403 Z_h^{0.8787} Z_{dr}^{-0.8077}$
$R_3 = 49.2144 K_{dp}^{0.9429} 10^{-0.2731 Z_{dr}}$
$R_4 = 25.2598 K_{dp}^{0.9951} Z_{dr}^{-0.6383}$
$R_5 = 20.47 K_{dp}^{0.75}$
$10\log(Z_h / R_6) = 18.9960 + 16.9758 Z_{dr}$ $- 9.4325 Z_{dr}^2 + 2.1542 Z_{dr}^3$

As shown, all the errors increase, particularly at low rainfall rates, with the algorithm R_1 having the smallest errors (less than 40%). For rainfall rates larger than around 40 mm hr^{-1}, algorithms R_3 and R_5 produced the smallest errors, which are around 10% smaller than algorithm R_1. This suggests that the use of an hybrid algorithm of the form R_1 for low rain rates (R<40 mm hr^{-1}) and of the form R_3 or R_5 for high rain rates (R>40 mm hr^{-1}) may be optimal. However, it is important to note that for rainfall rates less than about 40 mm hr^{-1}, algorithm R_1 has an error which is around 10-15% smaller than the conventional MP relationship. The remarkable improvement comes when the rainfall rate exceeds 40 mm hr^{-1}.

5 Results

In order to apply the algorithms shown in Table 1, it is necessary to keep the noise levels within the given ranges and any bias in the radar measurements has to be removed. Gorgucci et al., (1999) showed that Z_{dr} measurements in rain at 90° elevation are useful in removing any bias. Because large raindrops can be approximated by oblate spheroids, vertical pointing measurements of Z_{dr} are close to 0 dB. Any deviation from this value can be due to non-zero mean canting angle of raindrops, ground clutter and bias due to different gains in the H and V-polarised channels (Gorgucci et al., 1999). Fig. 3 shows vertical pointing measurements of Z_{dr} averaged from measurements obtained in rain during one hour. The mean average value over all the azimuth angles is around -0.03 dB (bias), but there is a cyclical variation of around 0.5 dB peak to peak. This variation depends on the azimuth angle and it can have a large effect on the rainfall estimation. The theoretical error plots shown in Fig. 2b were obtained assuming levels of noise in Z_{dr} of 0.1 dB, but the error plots can be larger than expected due to the azimuth-dependent variation of Z_{dr}. Therefore, this is an important point that has to be considered and it would be interesting to determine whether or not this cyclical variation can be removed.

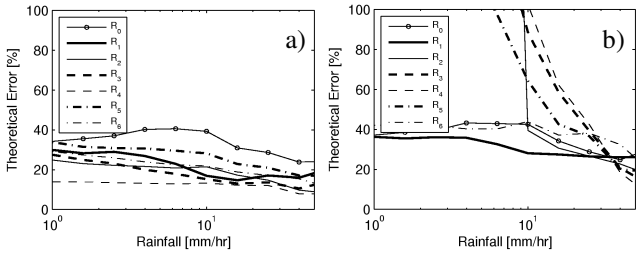

Fig. 2. Theoretical errors for the polarimetric rain estimator algorithms shown in Table 1. a) noise free and b) with noise.

The processing of the radar data was carried out as follows. The ground clutter and anomalous propagation echoes for two elevations (~0.5° and ~1.5°) were removed using a fuzzy algorithm, which uses most of the radar measurements. Then, a moving window average filter was applied to Z_h and Z_{dr} to reduce the standard error. The averaging was calculated avoiding non-meteorological echoes. The radar measurements Z_h and Z_{dr} corresponding to the rain gauge locations were extracted. If there were ground clutter contaminated pixels, then the next elevation was used. Thirty-min radar and rain gauge accumulations were used to perform the comparisons. Only the algorithms involving Z_h and Z_{dr} were tested. No attempt has been made to correct for attenuation because of the relatively low rain rates involved in the comparisons.

Table 2 shows the results of the comparisons for different averaging windows using the conventional MP equation and the algorithm R_1, which is the one that produced the best results. The criteria to evaluate the performance of the algorithms were the Root Mean Square Error (RMSE) and the normalised bias, which was defined as $< R_r - R_g > / < R_g >$, where R_r is the radar estimated rainfall, R_g is the gauge measurement and the brackets denote average values. Radar hydrologists are interested in rainfall rates producing flooding and therefore the data points used in the performance criteria were values of accumulated rain equal or larger than 1 mm. Table 2 shows that the MP relationship present lower RMSE compared to the polarimetric algorithm R_1. However, the MP relationship also produces the largest bias (negative sign is indicative of underestimation) compared to algorithm R_1.

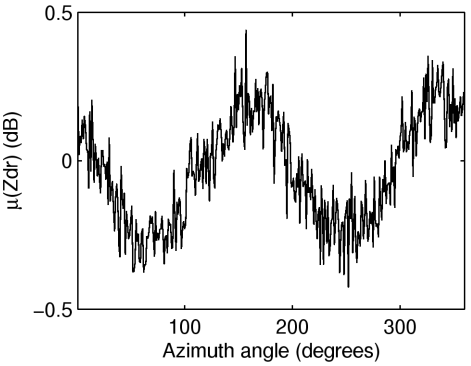

Fig. 3. Hourly averaged Z_{dr} measurements collected in rain at 90° elevation as a function of the azimuth (2.16 RPM on 24/05/2006).

Table 2. Root mean square errors and normalised bias for the MP relationship R_0 and the polarimetric algorithm R_1

	R_0		R_1	
Averaging	RMSE	BIAS	RMSE	BIAS
1.25 km x 1°	0.87mm	-21.59%	1.49mm	15.27%
2.25 km x 1°	0.84mm	-25.44%	1.11mm	7.09%
4.25 km x 1°	0.86mm	-30.77%	0.93mm	-1.91%
1.25 km x 3°	0.85mm	-25.36%	1.13mm	7.07%
2.25 km x 3°	0.85mm	-27.88%	0.95mm	2.46%
4.25 km x 3°	0.87mm	-32.28%	0.85mm	-5.03%

Algorithm R_1 performs better when increasing the size of the averaging window, showing an overall reduction of RMSE and normalised bias. This is because the standard error in Z_{dr} is reduced with the averaging. Fig. 4 shows the results of the comparisons using the conventional MP equation and algorithm R_1, for a particular averaging window of 4.25 km x 3°. As shown, although the RMSE is approximately the same in both algorithms, the normalised bias gives an extra measure of performance, with algorithm R_1 indicating less bias than the MP relationship.

6 Conclusions

Theoretical error plots for the different physically-based polarimetric rain rate algorithms that had been derived using non-linear regression among simulated radar measurements from measured DSD and assuming different raindrop shape models were compared to the MP relationship. For the noise-free case these showed that the dual-polarisation rain-rate results outperformed the MP results, particularly at high rain rates, but when theoretical levels of noise are added, only algorithm R_1 outperformed the MP relationship for all rain-rates and algorithms R_3 and R_5 outperformed the MP relationship for heavy rain.

A preliminary case study was presented using the derived polarimetric rain rate algorithms and precipitation events occurring over the Medway catchment. The results show that RMSE obtained with the MP relationship are slightly smaller than the polarimetric algorithm R_1, but the bias in the latter was smaller. The MP relationship tends to underestimate the heavy rain rates. Long-term radar gauge comparisons are needed to establish more accurately the performance of the proposed algorithms.

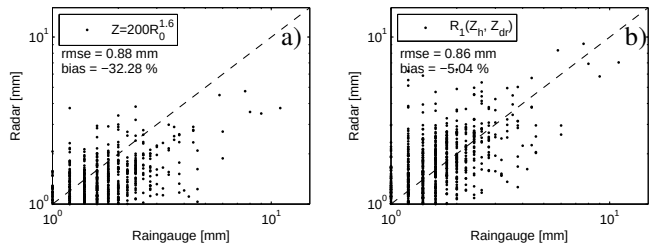

Fig. 4. Radar and rain gauge comparisons with an average window of 4.25 km x 3° over 30-min accumulations (19-27 May 2006).

Acknowledgements: The authors would like to acknowledge the financial support provided by the EPSRC Flood Risk Management Research Consortium (GR/S76304/01), the British Atmospheric Data Centre for providing disdrometer data, the UK Environment Agency (Michael Vaughan and Carla Richmond) for providing the rain gauge data and the UK Meteorological Office (Malcolm Kitchen and Jacqueline Sugier) for providing the C-band radar data.

References

Andsager, K., K, V. Beard, and N. L. Laird, 1999: Laboratory Measurements of axis ratios for large raindrops. *J. Atmos. Sci.*, **56**:2673-2683.

Atlas, D. and C. W. Ulbrich, 1977: Path- and area-integrated rainfall measurement by microwave attenuation in the 1-3 cm band. *J. Appl. Meteor.*, **16**:1322-1331.

Aydin, K. (2000) Centimeter and Millimiter Wave Scattering from Nonspherical Hydrometeors. In *Light scattering by nonspherical particles* by Mishchenko, M. I., J. W. Hovenier and L. D. Travis. Academic press.

Battan, L. J. (1973) *Radar observation of the atmosphere*. The University of Chicago Press.

Beard, K.V., and C. Chuang, 1987 A new model for the equilibrium shape of raindrops. *J. Atmos. Sci.*, **44**:1509–1524.

Bringi, V. N. and V. Chandrasekar, 2001: *Polarimetric Doppler Weather Radar, Principles and applications*. Cambridge University Press.

Chandrasekar, V. and V. N. Bringi, 1988: Error Structure of Multiparameter Radar and Surface Measurements of Rainfall. Part I: Differential Reflectivity, *J. Atmos. Oceanic Technol.,* **5**: 783-795.

Gorgucci, E., G. Scarchilli, and V. Chandrasekar 1999: A Procedure to Calibrate Multiparameter Weather Radar Using Properties of the Rain Medium. *IEEE Trans. Geosci. Remote Sensing*, **37**:269-276.

Holt, A. R., 1984: Some factors affecting the remote sensing of rain by polarization diversity radar in the 3- to 35 GHz frequency range. *Radio Science*, **19**:1399-1412.

Illingworth, A. J. and Stevens. C.J., 1987: An Optical Disdrometer for the Measurement of Raindrop Size Spectra in Windy Conditions. *J. Atmos. Oceanic Technol,* **4**:411–421.

Illingworth, A. J. and T. M. Blackman, 2002: The need to represent raindrop size spectra as normalized gamma distributions for the interpretation of polarization radar observations. *J. Appl. Meteor.*, **41**:286-297.

Lee, G. W., 2003: *Errors in rain measurement by radar: Effect of variability of drop size distributions*. Ph.D. thesis, McGill University, Montreal, Canada.

Marshall, J. S.,W. Hitschfeld, and K. L. S. Gunn, 1955: Advances in radar weather. *Advances in Geophysics*, **2**:1-56.

Mishchenko, M. I., J. W. Hovenier and L. D. Travis, 2000: *Light scattering by nonspherical particles*. Academic press.

Pruppacher, H. R. and K. V. Beard, 1970: A wind tunnel investigation of the internal circulations and shape of water drops falling at terminal velocity in air. *Quart. J. Roy. Meteor. Soc.*, **96**, 247-256.

Sachidananda, M. and Zrnic, D. S., 1987: Rain rate estimates from differential polarization measurements. *J. Atmos. Oceanic Technol.,* **4**:588-598.